

One Product, Two Pathways: Initially Divergent Radical Reactions Reconverge To Form a Single Product in High Yield

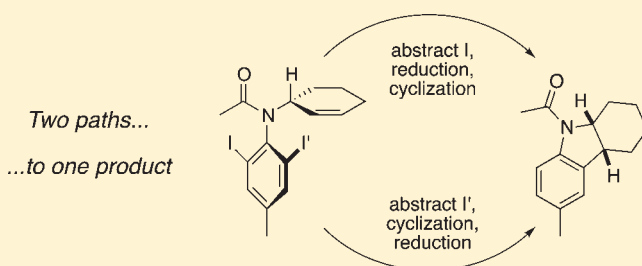
Achim Bruch,[†] Roland Fröhlich,[†] Stefan Grimme,[†] Armido Studer,^{*,†} and Dennis P. Curran^{*,‡}

[†]Organisch-Chemisches Institut, Westfälische Wilhelms-Universität, Corrensstrasse 40, 48149 Münster, Germany

[‡]Department of Chemistry, University of Pittsburgh, Pittsburgh, Pennsylvania 15260, United States

 Supporting Information

ABSTRACT: The paper describes examples of net diastereotopic-group-selective radical processes having the unusual feature that a single product is formed even though the key reaction of the two diastereotopic radical precursors is nonselective. For example, reaction of (*R*)-*N*-(cyclohex-2-en-1-yl)-*N*-(2,6-diiodo-4-methylphenyl)acetamide with tributyltin hydride produces 1-((4*aR*,9*aR*)-6-methyl-2,3,4,4*a*-tetrahydro-1*H*-carbazol-9(9*aH*)-yl)ethanone with high product selectivity and in high yield. Analysis of the concentration profiles of the closed-shell intermediates at the halfway point of the reaction shows that nonselective abstraction of diastereotopic iodides by tin radicals occurs, leading to diastereomeric aryl radicals. These isomeric intermediates evolve via two nonintersecting reaction pathways, cyclization and bimolecular trapping or vice versa, into the same final product. Origins of the selectivity are suggested on the basis of conformational analysis of the products using both X-ray crystallography and density functional theory calculations.



INTRODUCTION

In many multistep organic transformations, there is generally only one low-energy path to get from a precursor to a product. If the reaction wanders onto the wrong path, then it may not be possible to get back on track. Here we report a stereotopic-group-selective reaction that has two completely different paths to the same product. There are no U-turns, nor is it possible to go around the block; paths intersect nowhere but at their origin and destination. Despite that, it does not matter which path is taken; the same product is formed either way.

Stereotopic-group-selective reactions are generally performed in a direct manner by pitting two (or more) diastereomeric transition states (TSs) in competition with each other.¹ The product derived from the lower-energy TS, of course, wins the competition. This is illustrated in Figure 1 for the conversion of two diastereotopic groups X and X' in a precursor into different substituents A and B in a product.² The first group-selective reaction, here conversion of either X or X' to A, completely controls the overall stereoselectivity. The subsequent reaction with B occurs after the key selective step is over.

A long-held corollary to this type of reaction is that if the initial group-selective reaction occurs without selectivity, then the overall process cannot be selective. However, this corollary is not correct.

Some time ago, we recognized that a pair of stereotopic-group-selective reactions could be performed in a fundamentally different way that is based on reaction topography.^{3,4} By this method,

called stereoselection at the steady state, an apparent group-selective reaction can be accomplished in an indirect way by controlling the pathways by which nonselectively generated intermediates react.

Consider the divergence of the same precursor with X and X' to a pair of radicals and assume that this step occurs without selectivity (Figure 1, bottom). These intermediate radicals are diastereomers that can react differently. Now imagine that one diastereomer reacts with A before B while the other reacts with B before A. At the end, these divergent paths reconverge to the same product. A net group-selective reaction results even though there was no selectivity in the initial (and only) opportunity for direct differentiation of the two groups X and X'.

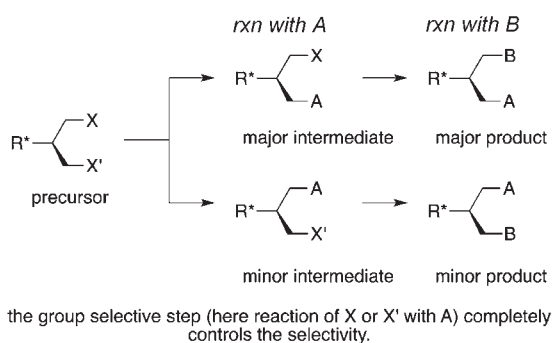
The direct and indirect processes differ in many ways,^{3b} one of the most important being the theoretical yield of the major product. In the case of the classical group-selective process, the yield of the major product can never exceed the level of stereoselectivity in the first step. In the steady-state process, the converging topography can in theory override the lack of group selectivity, providing a high yield of one product.

Reaction time course analyses of net diastereotopic-group-selective radical reactions have provided convincing evidence of the principle of stereoselection at the steady state; however, the selectivities observed to date have been low.^{4a} For example, reduction of diiodide **1** with Bu₃SnH at 0.7 M provides three

Received: August 1, 2011

Published: September 01, 2011

Direct (traditional) group selective transformation



Indirect group selectivity at the steady state

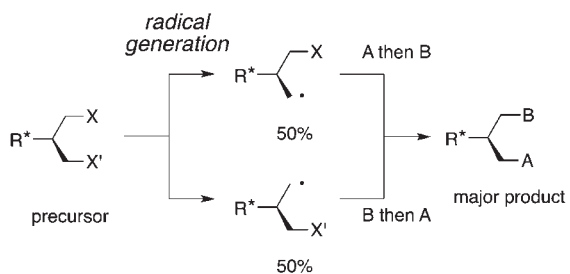


Figure 1. Direct (traditional) and indirect (steady-state) pathways for accomplishing a pair of net group-selective reactions with A and B. It is assumed that R* has an element of chirality that makes X and X' diastereotopic.

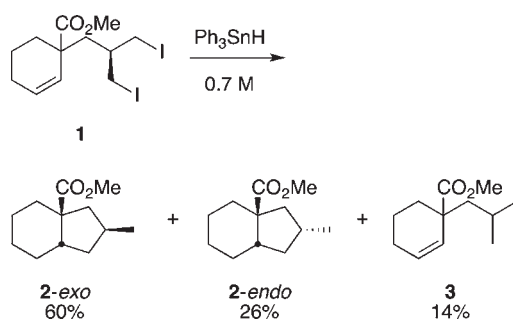


Figure 2. Typical example of product selection at the steady state involving a substrate **1** bearing two radical precursors and a prochiral center.

products, **2-exo**, **2-endo**, and **3**, in yields of 60, 26, and 14%, respectively (Figure 2). The abstraction of an iodine atom by tin radical to start this reaction is nonselective, yet the **2-exo/2-endo** ratio exceeds 1/1 and the yield of **2-exo** exceeds 50%. This occurs because one diastereomeric radical goes to **2-exo** by cyclization followed by reductive deiodination while the other goes by reductive deiodination followed by cyclization.

The object of this work was to discover examples of product selection at the steady state that occur with high selectivities. This was accomplished by using the same types of competing

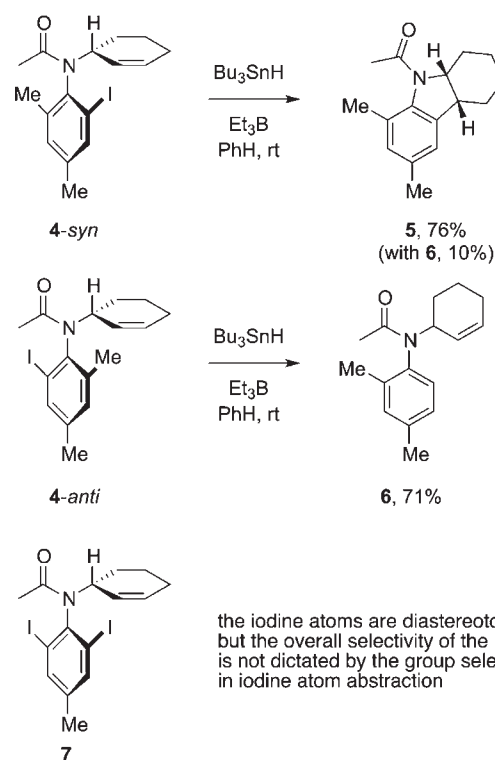


Figure 3. Precursor **7** designed on the basis of widely differing outcomes in radical reactions of atropisomers **4-syn** and **4-anti**.

reactions (cyclization and bimolecular trapping) but changing the prochiral element of substrates like **1** from a stereocenter into an axis.

RESULTS AND DISCUSSION

The opportunity to design a substrate for a highly selective process presented itself during seemingly unrelated work on radical reactions of axially chiral anilides.⁵ In particular, atropisomers **4-syn** and **4-anti** are separated by high rotational barriers of 36–37 kcal mol⁻¹ and can be readily obtained in pure form (Figure 3). Remarkably, atropisomer **4-syn** reacts with Bu₃SnH to give principally **5**, the product of cyclization followed by trapping, whereas atropisomer **4-anti** gives exclusively **6**, the intercepted product of direct trapping without cyclization. The direct-trapping product **6** was obtained even at relatively low concentrations of the tin hydride.

Evidently, there are large differences in the rates of cyclization of intermediate radicals derived from **4-syn** (fast) and **4-anti** (slow). To capitalize on these differences in a steady-state setting, we “fused” diastereomers **4-syn** and **4-anti** into a single precursor **7** bearing two iodine atoms at the 2- and 6-positions of the *N*-aryl ring. This compound shares a key feature of previously studied (but poorly selective) precursors in that it contains two diastereomeric radical precursors.^{4b} However, the overall process is different because the prochiral element of the precursor is a *N*–Ar axis (not a stereocenter) and because the net group selectivity is expressed as a ratio of constitutional isomers (reduced and cyclized) rather than stereoisomers.

Equation 1 shows the synthesis of the precursor. Diiodoanilide **7** was prepared by acylation of 2,6-diiodo-4-methylaniline

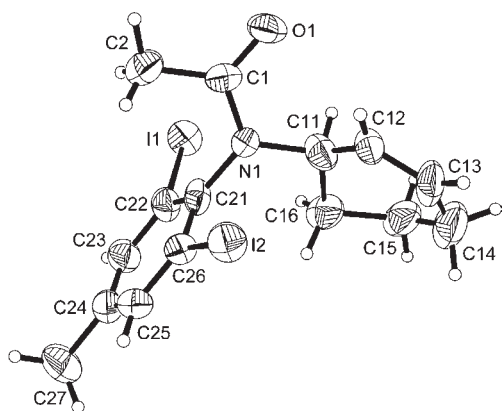
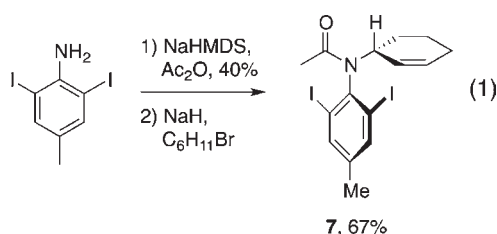


Figure 4. X-ray crystal structure of diiodide **7**. Selected torsion angles: O1–C1–N1–C21, -177.2° ; C1–N1–C21–C26, -90.6° ; C1–N1–C11–H11, -50.5° .

followed by allylation of the resulting product with cyclohexenyl bromide ($C_6H_{11}Br$) and base.



The X-ray crystal structure of **7** is shown in Figure 4. As expected from related molecules such as **4**, the planes of the amide and the aryl ring of **7** are virtually orthogonal. The barrier for rotation around the N–Ar bond cannot be directly measured because of the symmetry of the aryl ring substituents, but by analogy to **4** it must be well over 30 kcal/mol. Also, as in most anilides, the amide C2(O1)–N1 bond of **7** adopts the *E* geometry in both solution and the solid state.⁶ The amide nitrogen substituent adopts a pseudoequatorial position on the cyclohexenyl ring, and the amide plane is roughly staggered between the C11 substituents H11 and C12. This geometry is typical for amides with secondary-alkyl N-substituents and results from minimization of A-strain.⁷

To study the time-dependent concentration profiles of products and intermediates during a typical radical reaction, diiodide **7** was treated with Bu_3SnH (4.0 equiv) in the presence of the initiator 1,1'-azobis(cyclohexane-1-carbonitrile) (V-40, 0.2 equiv) in benzene at $80^\circ C$, and the reaction course was followed by GC analysis (Scheme 1 and Figure 5).

Authentic samples of the intermediate products **8** and **9** (one iodide reacted) and final products **10** and **11**⁹ (both iodides reacted) were synthesized as standards (see the Supporting Information). Isomers **8-syn** and **8-anti** exhibited a single peak upon GC analysis as a result of their rapid interconversion under the high-temperature conditions of the analysis (see below), so only a total amount of **8** was determined.

The two monodehalogenated intermediates **8** and **9** were identified after 16 min in **8** and 12% yield, respectively. The targeted final product **11** was already present in 11% yield at that time. The yields of **8** and **9** soon rose to just over 15%, remained nearly constant for a time, and then diminished. Meanwhile, the starting diiodide **7** was consumed, and the final product **11** was

Scheme 1. Structures of the Intermediate (**8** and **9**) and Final (**10** and **11**) Products Formed during the Tin Hydride Reduction of **7**

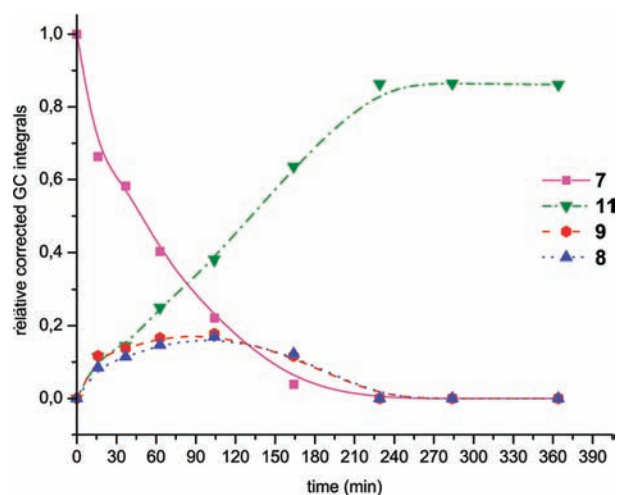
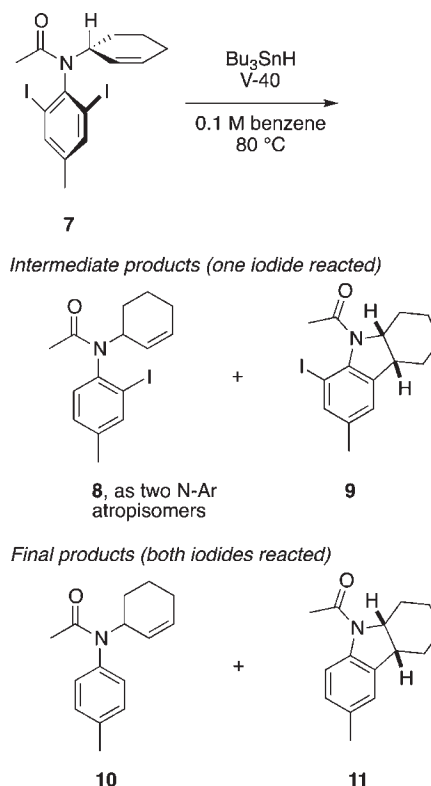
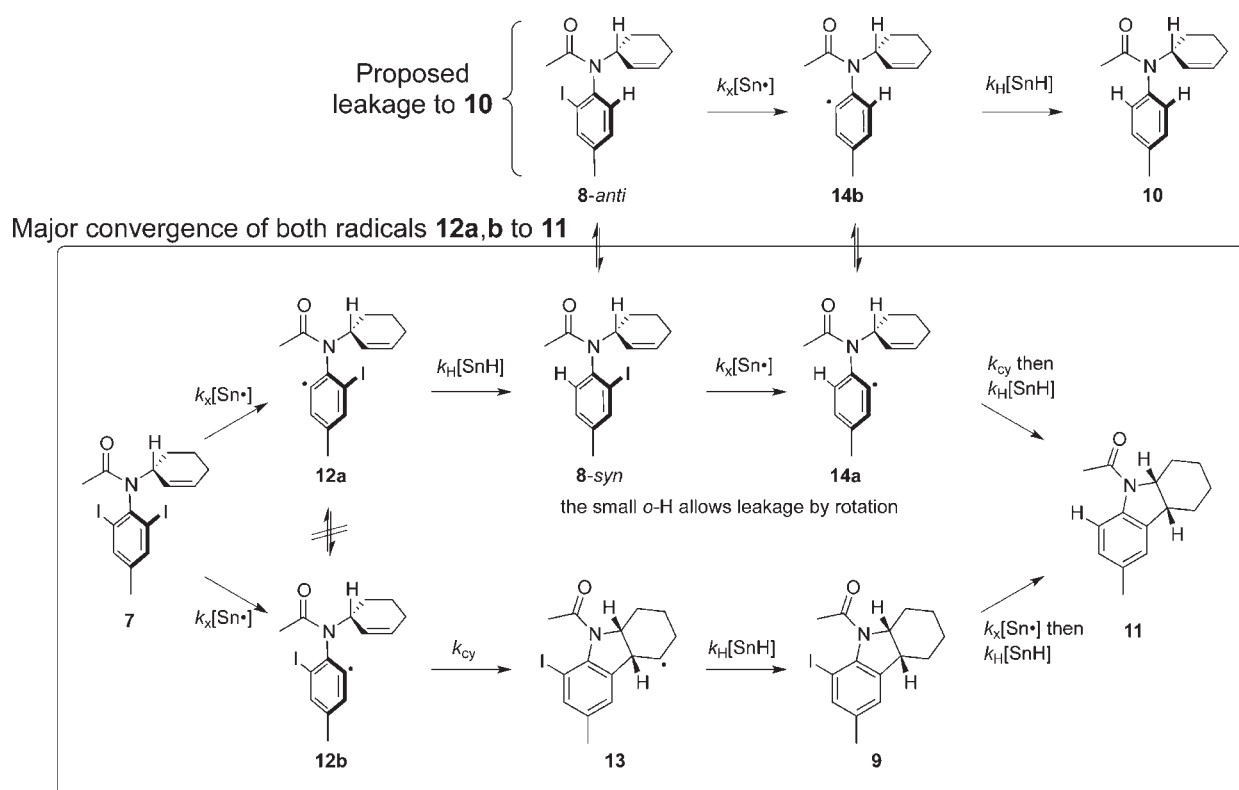


Figure 5. Concentration profiles of major products in the Bu_3SnH -mediated reaction of diiodoanilide **7**.

eventually formed in high yield. The reaction was complete after 4 h, and the major product **11** was formed in 86% GC yield along with a small amount of doubly reduced anilide **10** (5%).⁸ The outcome is far superior to prior examples of product selection at the steady state in terms of both yield (86%) and selectivity (94/6) of the major product, **11**.

The observed time-course profiles in Figure 5 conforms well with that expected on the basis of the kinetic theory that follows



The minor convergence (not shown) is entered if radical **12a** cyclizes or if radical **12b** is reduced by tin hydride

Figure 6. Simplified mechanistic analysis of the tin hydride reduction of **7** showing the “major convergence” to **11** and a proposed leakage to the doubly reduced product **10**.

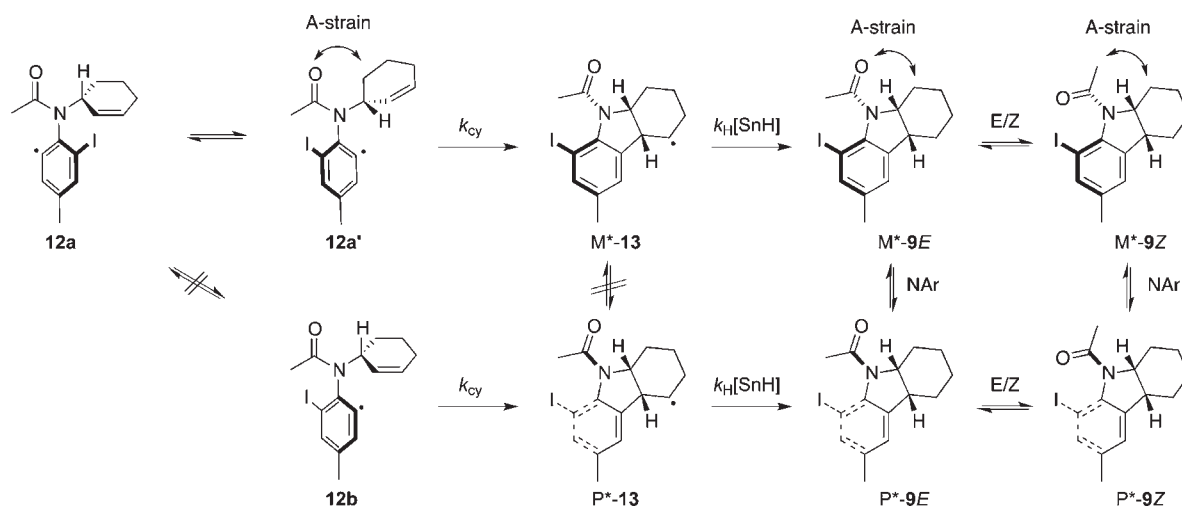


Figure 7. Assessment of the importance of residual axial chirality in the cyclizations of radicals **12** along with four possible conformations of product **9**.

from the simplified mechanistic framework shown in Figure 6. Product selection at the steady state is complex because all of the intermediates and products can arise from two partially interconnected pathways, a major convergence and a minor convergence.^{3a} Conveniently, we can neglect the minor convergence for the analysis in Figure 6 because the process is so selective (Figure S1 in the Supporting Information shows all of the pathways.)

Paths diverge immediately with abstraction of either the α - or β -oriented iodine atom from **7** by $\text{Bu}_3\text{Sn}\cdot$ to provide the two

diastereomeric radicals **12a** and **12b**. That this diastereotopic-group-selective process occurs without selectivity is shown by the observation of equal amounts of the immediately downstream products **8** and **9** derived from these radicals throughout the reaction. Radical **12b** resembles the radical derived from 4-*syn* in Figure 3, so it cyclizes very rapidly to provide **13**, which in turn delivers **9** by hydrogen atom abstraction. In contrast, radical **12a** resembles the radical derived from 4-*anti* in Figure 3, so it does not cyclize and instead is reduced to **8-syn**. This part of the

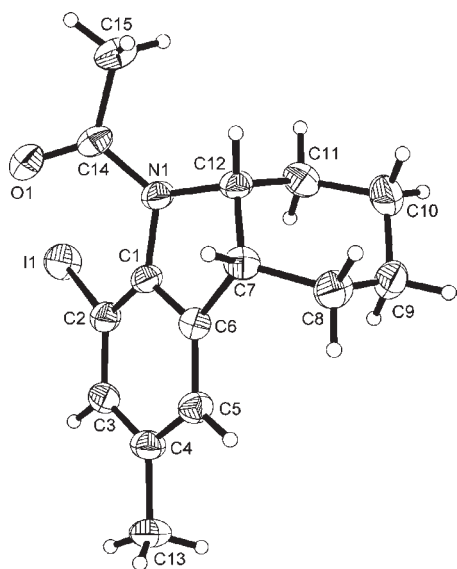


Figure 8. X-ray crystal structure of P^{*}-9Z. Selected torsion angles: O1–C14–N1–C1, 6.5°; C14–N1–C1–C2, –50.8°; C14–N1–C12–H12, –4.0°.

process is an example in which stereoisomeric precursors (**12a** and **12b**) subjected to identical reaction conditions give constitutionally different products (**8** and **9**) rather than stereoisomeric products.¹⁰

From there, the roles are reversed; abstraction of iodine from **9** now gives a radical that cannot again cyclize and thus is reduced, while radical **14a** derived from **8** is very similar to **12b** and rapidly cyclizes prior to reduction. The net result is that the pathways reconverge to give the same product **11** in high yield. In short, if one diastereotopic iodine of **7** is abstracted, then cyclization precedes direct reduction. If the other is abstracted, then direct reduction followed by cyclization occurs.

The high selectivity for formation of **11** may seem surprising since aryl radicals **12a** and **12b** must react with tin hydride with virtually the same rate constant.¹¹ However, because the process occurs at the steady state and the cyclization of **12b** is much faster than **12a**, the concentration of **12a** must always greatly exceed that of **12b**. This concentration gradient ensures that tin hydride reacts with **12a** and not with **12b**. Though the end result is selectivity of two constitutional isomers (**10** and **11**), there is a hidden yet crucial feature of stereoselectivity. In principle, radical **12a** can cyclize. But if it were to do so, it would not give the same radical **13** resulting from cyclization of **12b** because the N–Ar axis cannot rotate in competition with cyclization.

The consequences of the prostereogenic axis in **7** for the radical cyclization are explored in Figure 7. Radical **12b** (lower line of structures) is well-positioned to cyclize with simple twisting of the N–Ar bond and the allylic C–N bond to bring the radical and the alkene together. However, this does not provide a “flat” five-membered ring in product **13** (as suggested by the simplified structures in Figure 6) but instead one with residual axial chirality, as shown in P^{*}-**13** (Figure 7).^{12,13}

In contrast, radical **12a** (upper line of structures in Figure 7) is not well-positioned to cyclize until the allylic C–N bond rotates substantially, with an attendant increase in A-strain. Cyclization through a conformer like **12a'** now gives a product M^{*}-**13** with axial chirality opposite that of P^{*}-**13**. In other words, the immediate

result of the two cyclizations is the formation not of the same radical **13** but of the diastereomeric radicals M^{*}-**13** and P^{*}-**13**.

The ultimate closed-shell products **9** from reduction of these radicals can presumably interconvert thermally because the newly formed ring lowers the barrier to N–Ar rotation (now associated with a conformational change of the five-membered ring). Also, the amide C–N bond can rotate between *E* and *Z*.^{12,13} This results in the four conformers of **9** shown in Figure 7. However, these rotation processes occur after all of the action with the radicals is over.

Efforts to study **9** by NMR spectroscopic analysis were complicated by the presence of overlapping broad peaks that could not be unambiguously assigned to the candidate rotamers. However, we were able to solve the X-ray crystal structure of **9**, and this is shown in Figure 8.

The crystal exhibited only conformer P^{*}-9Z, in which the cyclohexyl ring exists in a chair conformation with the nitrogen substituent occupying a pseudoequatorial position and the aryl substituent a pseudoaxial position. This (*Z*)-amide rotamer cannot be the primary product of the radical cyclization. The residual axial chirality of the N–Ar-bond is clearly visible in the X-ray structure (bridgehead H atoms and the I atom anti to each other). At about 50°, the N–Ar twist angle is reduced relative to that precursor **7** but is still substantial. The amide C–N bond now nearly eclipses the former allylic C–H bond (H12), thus avoiding A-strain between the methyl group of the acyl substituent (C15) and the methylene group (C11) of the cyclohexyl ring.

Loosely related amides exhibit both *E* and *Z* rotamers in solution, with the *E* rotamer often being favored.^{12,13} We were not confident that the crystal structure provided the favored ground-state amide rotamer. Although it seems less likely (based on A-strain), we also considered that the N–Ar twist direction in the crystal structure might also not be favored in the ground state.

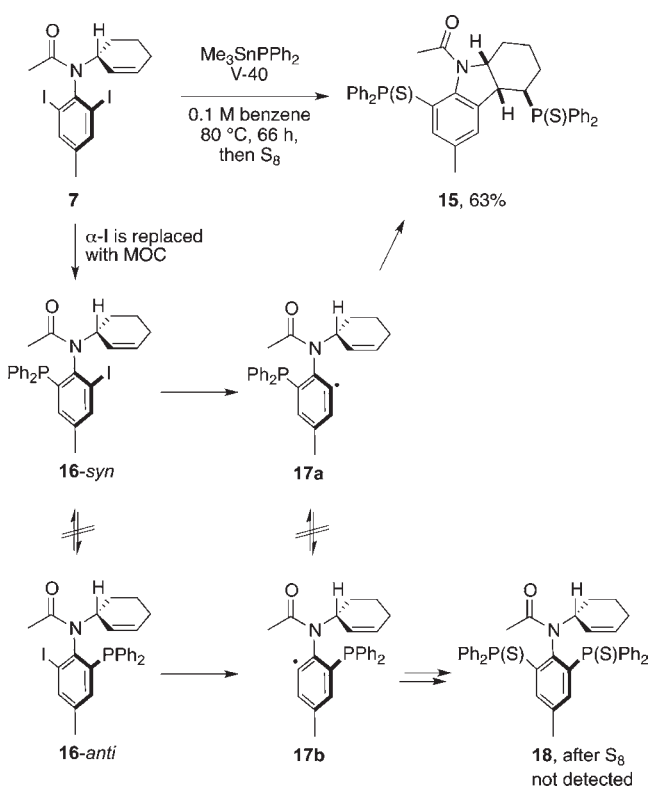
To address these issues, the conformational space of **9** with respect to the axial chirality (torsion around the C_{Ar}–N bond vector) and rotation of the acetyl groups was explored by state-of-the-art dispersion-corrected density functional theory (DFT) at the DSD-BLYP-D3/def2-QZVP//TPSS-D3/def2-TZVP level.¹⁴ Details of the calculations and absolute energies (in hartrees) as well as coordinates of geometry-optimized structures are provided in the Supporting Information.

In the gas phase, the relative free energies Δ*G*(298 K) are 0.0 kcal/mol for P^{*}-9E, 0.96 kcal/mol for P^{*}-9Z, 8.66 kcal/mol for M^{*}-9E, and 7.26 kcal/mol for M^{*}-9Z (for the structures, see Figure 7). In all of the structures, the cyclohexane ring is in the same chair-type conformation.

When corrections for the solvent (chloroform) were included, the Δ*G*(298 K) values for P^{*}-9E (0.0 kcal/mol) and P^{*}-9Z (–0.19 kcal/mol) were reversed, but the N–Ar twist isomers M^{*}-9E (8.86 kcal/mol) and M^{*}-9Z (6.65 kcal/mol) remained much higher in energy. The reversal to favor P^{*}-9Z slightly in solution results from the larger dipole moment (by about 1.3 D) of P^{*}-9Z relative to P^{*}-9E. Thus, it seems likely that substantial amounts of both P^{*}-9E and P^{*}-9Z are present in solution and that the *Z* rotamer selectively crystallizes.

The high relative energy of M^{*}-9E with respect to P^{*}-9E (7–9 kcal/mol) is consistent with the notion that M^{*}-9E must deal with significant A-strain issues because the N–Ar twist direction and the stereocenter configurations are mismatched. The same mismatching is present in the cyclized radical M^{*}-**13** in comparison with P^{*}-**13**. Because of the developing strain, the activation

Scheme 2. Radical Cyclization and Trapping Mediated by $\text{Me}_3\text{SnPPh}_2$



energy for the cyclization of **12a'** leading to $\text{M}^*\text{-13}$ must be far higher than the activation energy for cyclization of **12b** to $\text{P}^*\text{-13}$. Neither cyclization nor N–Ar rotation of aryl radical **12a** or **12a'** can compete with bimolecular tin hydride reduction, so **12a** is funneled selectively into **8-syn**, as observed in the experiment (see the concentration profiles of the intermediates in Figure 5).

In short, the overall transformation changes from a stereoselective one to a product-selective one (**11/10** ratio) because the difference ratio of cyclization of isomeric radicals **12a** and **12b** is so high that effectively no minor stereoisomer results from **12a**.

What is the origin of the doubly reduced product **10**? In principle, this could arise from a leakage into the minor convergence at one of several branch points. For example, if radical **12b** leaks by reduction with tin hydride rather than cyclization, then the resulting product will probably also be reduced, giving **10** (see Figure S1 in the Supporting Information). However, this seems unlikely on the basis of the cyclization results with **4** and related *o*-iodoanilides.

Prior measurements of the rotational barrier and cyclization experiments with **7** and **8** suggest a different explanation for the origin of **10**. Reduction of **12a** by tin hydride should occur with memory of axial chirality to produce only **8-syn**,^{5b} but the attendant replacement of the iodine atom by hydrogen reduces the rotational barrier for interconversion of **8-syn** and **8-anti** to 23–24 kcal mol⁻¹.^{5a} At 80 °C, rotation of the N–Ar bond of **8** is probably competitive to some extent with onward radical generation. In addition, the previous results suggest that radicals **14a** and **14b** might also partially equilibrate.^{5a} However, radical **14b** is of the slow-cyclizing variety, so the return back to the major convergence is the more likely of the two rotations here.

If this notion is correct, then the leaks at both the closed-shell (**8**) and open-shell (**14**) intermediates can be plugged by using a radical-trapping agent that is larger than a hydrogen atom. Aryl radicals react with $\text{Me}_3\text{SnPPh}_2$ at rates similar to those with Bu_3SnH ,^{5b,15} so transformation of **7** to a major double-phosphorylated product should be feasible.

To this end, we treated **7** with $\text{Me}_3\text{SnPPh}_2$ (6.0 equiv) and initiator V-40 in benzene (Scheme 2). To simplify the analysis and product isolation, the reaction mixture was treated with S_8 to afford bis(phosphine sulfide) **15**, which was isolated in 63% yield after chromatography. The transfer of a phosphine group rather than a hydrogen atom provides a third stereocenter in the cyclohexyl ring of the product **15**. This traditional face-selective reaction of a radical also occurs with complete stereoselectivity by reaction from the less hindered exo face of the adjacent bicyclic ring fusion.¹⁶

The structure of **15** was determined by X-ray analysis (see Figure S5 in the Supporting Information), which confirmed the relative configuration of the new stereocenter. Otherwise, the structure of **15** was similar to that of **9** in three key aspects: (1) the (*Z*)-amide rotamer was present; (2) the N–Ar twist angle was substantial (45°); and (3) the amide C–N bond roughly eclipsed the adjacent cyclohexyl C–H bond. These features reinforce the stereochemical analysis in Figure 7.

The double phosphorylation is not as clean and high-yielding as the tin hydride-mediated reaction, and minor side products resulting from monophosphorylation were detected (see the Supporting Information). These side products are common in aryl radical phosphorylation,^{5b,15} and their amounts can be reduced to <10% by using a relatively high concentration of $\text{Me}_3\text{SnPPh}_2$ (0.1 M). Importantly, we looked by both GC analysis and ³¹P NMR spectroscopy but were not able to identify the double-trapped side product **18** that is analogous to **10**.

The absence of **18** can be understood by the partial mechanistic analysis shown in the lower part of Scheme 2. Abstraction of the β -iodine atom from **7** is not shown because it follows a path directly analogous to that in Figure 6; cyclization is followed by phosphorylation to give **15**. Abstraction of the α -iodine atom gives the aryl radical that does not cyclize and instead is phosphorylated with memory of axial chirality (MOC)^{5b} to give **16-syn**. Now this closed-shell intermediate has two large ortho substituents, so the N–Ar bond cannot rotate to give **16-anti** in competition with onward reaction, even at 80 °C. Abstraction of the remaining iodine atom from **16-syn** provides radical **17a**, whose cyclization is faster than rotation to **17b** again because of the presence of the larger Ph_2P substituent. In short, phosphorylation plugs both potential leaks.

CONCLUSIONS

We have developed a high-yielding and highly selective process for the formation of cyclized products such as **11** and **15** from substrate **7** containing diastereotopic radical precursors. This transformation is founded on the concept of product selection at the steady state. In classical group-selective processes, the maximum yield of a major product is fixed in the initial group-selective step. If there is no selectivity in this step, then a product yield cannot exceed 50%. In essence, there is one path from the precursor to the product, so a wrong turn at the group-selection step cannot be tolerated.

At the steady state, the initial group selectivity plays only a supporting role. The lead role is played by the reaction topology

because there are two main paths to the product. If one diastereotopic iodine atom is abstracted in the first step, then the system follows one path to the product. Abstraction of the other iodine atom might initially appear to be a wrong turn, but instead the product is simply reached by the other path. In essence, the system is self-correcting provided that the kinetics are in order to prevent any of several other possible wrong turns along the way.

This unusual case of reaction selectivity has been demonstrated on aryl radical cascades comprising cyclization and bimolecular trapping. The net result is product selection between two constitutional isomers (reduced and cyclized), and high yields of cyclized products are obtained. However, underlying this outcome is a key aspect of stereoselectivity. The initial rotationally isomeric radicals **12** cyclize not to the same product at different rates but instead to different products (N–Ar twist isomers **13**) at different rates. One of these stereoisomeric products is so high in energy that the radical cyclization producing it cannot compete at all with bimolecular reduction.

The ability to map out two separate, nonintersecting pathways to the same destination is a feature of the steady state, not of radical reactions per se. Therefore, the principles of product selection outlined herein are applicable in other areas such as catalysis where reactive intermediates are involved.

■ ASSOCIATED CONTENT

S Supporting Information. Experimental procedures and compound characterization data. This material is available free of charge via the Internet at <http://pubs.acs.org>.

■ AUTHOR INFORMATION

Corresponding Author

studer@uni-muenster.de; curran@pitt.edu

■ ACKNOWLEDGMENT

We thank the DFG and the National Science Foundation for support of the work in Germany and the U.S., respectively. D.P.C. thanks the Humboldt Foundation for a Senior Research Fellowship.

■ REFERENCES

- (1) Eliel, E. L.; Wilen, S. *Stereochemistry of Organic Compounds*; Wiley-Interscience: New York, 1994.
- (2) The analysis assumes that there are no additional reactions outside of those shown.
- (3) (a) DeMello, N. C.; Curran, D. P. *J. Am. Chem. Soc.* **1998**, *120*, 329–341. (b) Curran, D. P.; Qi, H. Y.; DeMello, N. C.; Lin, C. H. *J. Am. Chem. Soc.* **1994**, *116*, 8430–8431.
- (4) (a) Curran, D. P.; Lin, C. H.; DeMello, N.; Junggebauer, J. *J. Am. Chem. Soc.* **1998**, *120*, 342–351. (b) Andrukiewicz, R.; Cmoch, P.; Gawel, A.; Staliński, K. *J. Org. Chem.* **2004**, *69*, 1844–1848. (c) Stalinski, K.; Curran, D. P. *J. Org. Chem.* **2002**, *67*, 2982–2988.
- (5) (a) Guthrie, D. B.; Geib, S. J.; Curran, D. P. *J. Am. Chem. Soc.* **2011**, *133*, 115–122. (b) Bruch, A.; Ambrosius, A.; Fröhlich, R.; Studer, A.; Guthrie, D. B.; Zhang, H.; Curran, D. P. *J. Am. Chem. Soc.* **2010**, *132*, 11452–11454.
- (6) (a) Stewart, W. E.; Siddall, T. H. *Chem. Rev.* **1970**, *70*, 517–551. (b) Curran, D. P.; Hale, G. R.; Geib, S. J.; Balog, A.; Cass, Q. B.; Degani, A. L. G.; Hernandez, M. Z.; Freitas, L. C. G. *Tetrahedron: Asymmetry*

1997, *8*, 3955–3975. (c) Itai, A.; Toriumi, Y.; Saito, S.; Kagechika, H.; Shudo, K. *J. Am. Chem. Soc.* **1992**, *114*, 10649–10650.

- (7) Hoffmann, R. W. *Chem. Rev.* **1989**, *89*, 1841–1860.
- (8) Traces of two unidentified byproducts (7% and 2%) accounted for the balance of the starting material.
- (9) According to NMR analysis, final product **11** was a 78:22 mixture of amide C–N rotamers. The proton in the position ortho to the nitrogen atom of the major rotamer showed a downfield shift of about 1.0 ppm relative to the other signals of the aromatic protons. This may have been caused by the proximity of the carbonyl group to this proton in the Z isomer, and this isomer can be tentatively assigned as the predominant one.
- (10) (a) Kagan, H. B. *Croat. Chem. Acta* **1996**, *69*, 669–680. (b) Kumar, R. R.; Kagan, H. B. *Adv. Synth. Catal.* **2010**, *352*, 231–242.
- (11) Chatgililoglu, C.; Newcomb, M. *Adv. Organomet. Chem.* **1999**, *44*, 67–112.
- (12) (a) Tabata, H.; Nakagomi, J.; Morizono, D.; Oshitari, T.; Takahashi, H.; Natsugari, H. *Angew. Chem., Int. Ed.* **2011**, *50*, 3075–3079. (b) Takahashi, H.; Wakamatsu, S.; Tabata, H.; Oshitari, T.; Harada, A.; Inoue, K.; Natsugari, H. *Org. Lett.* **2011**, *13*, 760–763.
- (13) Keller, A. I. Ph.D. Thesis, University of Pittsburgh, Pittsburgh, PA, 2007; <http://etd.library.pitt.edu/ETD/available/etd-04122007-142347/>
- (14) (a) Kozuch, S.; Gruzman, D.; Martin, J. M. L. *J. Phys. Chem. C* **2010**, *114*, 20801–20808. (b) Goerigk, L.; Grimme, S. *J. Chem. Theory Comput.* **2011**, *7*, 291–309. (c) Goerigk, L.; Grimme, S. *Phys. Chem. Chem. Phys.* **2011**, *13*, 6670–6688. (d) Grimme, S.; Antony, J.; Ehrlich, S.; Krieg, H. *J. Chem. Phys.* **2010**, *132*, No. 154104. (e) Grimme, S.; Ehrlich, S.; Goerigk, L. *J. Comput. Chem.* **2011**, *32*, 1456–1465. (f) Weigend, F.; Furche, F.; Ahlrichs, R. *J. Chem. Phys.* **2003**, *119*, 12753–12762. (g) Schäfer, A.; Huber, C.; Ahlrichs, R. *J. Chem. Phys.* **1994**, *100*, 5829–5835. (h) Weigend, F.; Ahlrichs, R. *Phys. Chem. Chem. Phys.* **2005**, *7*, 3297–3305.
- (15) Vaillard, S. E.; Mück-Lichtenfeld, C.; Grimme, S.; Studer, A. *Angew. Chem., Int. Ed.* **2007**, *46*, 6533–6536.
- (16) Curran, D. P.; Porter, N. A.; Giese, B. *Stereochemistry of Radical Reactions: Concepts, Guidelines, and Synthetic Applications*; VCH: Weinheim, Germany, 1996.